

Pre-inflationary dynamics in loop quantum cosmology: Power-law potentials

M. Shahalam¹ *, Manabendra Sharma¹ †, Qiang Wu¹ ‡, and Anzhong Wang^{1,2} §

¹*Institute for Advanced Physics & Mathematics, Zhejiang University of Technology, Hangzhou, 310032, China*

²*GCAP-CASPER, Department of Physics, Baylor University, Waco, TX, 76798-7316, USA*

(Dated: July 23, 2018)

In this paper, we study the pre-inflationary dynamics for the power-law potential ($V(\phi) \propto \phi^n$) with $n < 2$ in the framework of loop quantum cosmology. In the case where the kinetic energy of the inflaton dominates at the initial, the evolution of the universe can always be divided into three different phases prior to reheating: *bouncing, transition and slow-roll inflation*. During the bouncing phase, the evolution of the expansion factor is independent not only on the initial conditions but also the inflationary potentials, and is given explicitly by an analytical solution. In contrast, for the potential energy dominated initial conditions, this universality is lost. We also obtain total number of e-folds during the slow-roll inflation, whereby physically viable models are identified. In addition, we present phase space analysis for the inflationary potentials under consideration and compare our results with the ones obtained previously for different potentials.

I. INTRODUCTION

The cosmic inflation resolves many problems in the standard model of cosmology such as the horizon and flatness problems, etc. Inflation also describes the formation of the large scale structure of the universe and the origin of inhomogeneities observed in the cosmic microwave background (CMB) [1]. There are large number of inflationary models that can be compatible with the observations. Recently, Planck 2015 results show that, in the case of a single field inflation, the simple quadratic potential model with ($V(\phi) \propto \phi^n$ with $n = 2$) is moderately disfavored in comparison to the power-law with $n < 2$ and Starobinsky potentials [2]. To this effect, it increases the curiosity in studying a single field inflation for the power-law potential with $n < 2$.

Despite the huge success of the standard inflationary models that are based on classical general relativity (GR), its past is insufficient due to the existence of a big bang singularity. It occurs in all scalar field models of inflation. To explain the inflationary process in context of GR, the initial singularity is inevitable [3, 4], with which it is not very clear when and how to set the initial conditions. Additionally, to be compatible with the present observations, the universe has to expand at least 60 e-folds during the inflation. Nevertheless, there are more than 70 e-folds during inflation in a large class of inflationary models [5]. In such models, the size of the present universe is less than that of the Planck at the beginning of inflation. As a result, the usual semi-classical treatments during inflation are questionable. This is known as the trans-Planckian problem [6, 7]. In addition, one normally ignores the pre-inflationary dynamics and sets the Bunch-Davies (BD) vacuum state at the time when

the wavelength of fluctuations were inside the Hubble horizon during inflation. However, the pre-inflationary dynamics can give rise to non-BD states at the onset of inflation [8].

To address the above important issues, one way is to work in the framework of loop quantum cosmology (LQC), which provides a viable description of inflation together with its pre-inflationary dynamics [8–11]. It is interesting to note that in such a framework the quantum geometrical effects at Planck scale provide a natural resolution of the big bang singularity [12–15], and the initial singularity is simply replaced by a nonsingular quantum bounce. Even more interesting, the universe which commences at the bounce can finally lead to the desired slow-roll inflation [16–24].

To study the pre-inflationary dynamics and cosmological perturbations, there are mainly two different approaches, the dressed metric [10, 25–27] and deformed algebra [28–33]. However, as far as only the evolution of the background of the universe is concerned, both approaches provide the same set of dynamical equations for the evolution of the background. Therefore, the results to be presented in this paper will be applicable to both approaches. With this in mind, we shall compare our results with the quadratic and Starobinsky potentials [8, 17, 19, 23]. In addition, similar analysis can be carried out for other inflationary models, such as, the monodromy, natural inflationary models, and so on. However, it is expected that the main conclusions obtained in this paper will be valid in those models, too, at least in the case in which the evolution of the universe is initially dominated by the kinetic energy of the inflaton [8]. This is because the kinetic energy will dominate the evolution of the universe in the whole bouncing phase, once it dominates it at the initial moment, and the potential energy remains un-dominant until the transition phase, at which the kinetic energy suddenly drops below the potential energy, whereby the latter takes over, and slow-roll inflation starts [8].

The rest of the paper is organized as follows. Section II is devoted to the detailed analysis of the background

*E-mail address: shahalam@zjut.edu.cn

†E-mail address: manabendra@zjut.edu.cn

‡E-mail address: wuq@zjut.edu.cn

§E-mail address: Anzhong_Wang@baylor.edu

evolution in the context of the positive inflaton velocity (PIV, $\dot{\phi} > 0$) and negative inflaton velocity (NIV, $\dot{\phi} < 0$), and also kinetic energy dominated (KED) and potential energy dominated (PED) cases at the quantum bounce. In section III, we present the phase space analysis for the power-law potential with $n < 2$. Our results are summarized in section IV.

Before proceeding further, we would like to notice that inflation with a power-law potential has been studied in Einstein's theory of gravity [34, 35] and in string-inspired model [36]. In particular, it was shown that weak singularity always occurs in high-order derivatives of the scalar field $|d^{(k+2)}\phi/dt^{k+2}| \rightarrow \infty$ as $\phi \rightarrow 0$ for $k < n < k + 1$, where k is an integer [35]. In particular, for $0 < n < 1$ the first derivative of the Ricci scalar diverges, $\dot{R} = 6(4H\dot{H} + \ddot{H}) \rightarrow -\infty$ as $\phi \rightarrow 0$. However, this singularity is weak in the sense that the space-time is geodesically complete and extendible at the singularity [35]. Since the Klein-Gordon equation in both cases are the same, it can be shown that such singularities also occur here in LQC. Moreover, recently inflation for a Bianchi I universe with different inflaton potentials and initial conditions were studied in [37], and interesting results were obtained.

II. EQUATIONS OF MOTION AND BACKGROUND EVOLUTION

In a spatially flat Friedmann-Lemaitre-Robertson-Walker (FLRW) universe, the modified Friedmann equation in the framework of LQC can be written as [38]

$$H^2 = \frac{8\pi}{3m_{pl}^2} \rho \left(1 - \frac{\rho}{\rho_c}\right) \quad (1)$$

where $H = \dot{a}/a$, represents the Hubble parameter, and dot denotes derivative with respect to the cosmic time t , m_{pl} is the Planck mass, ρ denotes the energy density of matter sources and ρ_c is the critical energy density that designates the maximum value of energy density and found to be $\rho_c \simeq 0.41m_{pl}^4$ [39, 40].

In the framework of LQC, the conservation equation remains the same as in the classical theory,

$$\dot{\rho} + 3H(\rho + p) = 0 \quad (2)$$

where p is the pressure of the matter field. If the matter source is a single scalar field, then the above equation gives the Klein-Gordon equation,

$$\ddot{\phi} + 3H\dot{\phi} + \frac{dV(\phi)}{d\phi} = 0 \quad (3)$$

Equation (1) shows that when $\rho = \rho_c$, the Hubble parameter becomes zero which means quantum bounce occurs at $\rho = \rho_c$. In the literature, the background evolution with the bouncing phase has been extensively discussed. One of the important result is that, following

bounce, a desired slow-roll inflation is obtained generically [8, 12, 17–19, 41]. Following this, we shall study “bounce and slow-roll” with the power-law potentials,

$$V(\phi) = \frac{1}{2}m^{4-n}\phi^n \quad (4)$$

where m has the dimension of mass. We consider five particular values of n : $n = 7/4, 4/3, 1, 2/3$ and $1/3$, respectively, which are all consistent with Planck 2015 results for inflationary universe [2]. The corresponding values of m for every potential are given as

$$\begin{aligned} m &= 6.2 \times 10^{-6} m_{pl}, & n &= 7/4, \\ &5.1 \times 10^{-5} m_{pl}, & n &= 4/3, \\ &1.9 \times 10^{-4} m_{pl}, & n &= 1, \\ &4.7 \times 10^{-4} m_{pl}, & n &= 2/3, \\ &1.1 \times 10^{-3} m_{pl}, & n &= 1/3. \end{aligned} \quad (5)$$

Let us first investigate the evolution equations numerically for different power-law potentials. We solve equations (1) and (3) numerically with the initial conditions of $a(t)$, $\phi(t)$ and $\dot{\phi}(t)$ at a particular moment. A natural choice of the time is at the bounce $t = t_B$, at which we have

$$\begin{aligned} \rho_B &= \rho_c = \frac{1}{2}\dot{\phi}^2(t_B) + V(\phi(t_B)), \\ \dot{a}(t_B) &= 0, \end{aligned} \quad (6)$$

which implies that

$$\dot{\phi}(t_B) = \pm \sqrt{2(\rho_c - V(\phi(t_B)))}, \quad (7)$$

and a suitable choice for $a(t_B)$ is

$$a(t_B) = 1. \quad (8)$$

Here after, we read off $\phi(t_B)$ and $\dot{\phi}(t_B)$ as ϕ_B and $\dot{\phi}_B$. Since $\dot{\phi}(t_B)$ is given by Eq.(7) for any given potential, the initial conditions will be uniquely specified by ϕ_B only. Following this, we shall consider two cases: (a) PIV: $\dot{\phi}_B > 0$ and (b) NIV: $\dot{\phi}_B < 0$. Let us introduce the following quantities which are important for this paper [8].

(1) The equation of state (EOS) $w(\phi)$ for inflaton field is given by

$$w(\phi) = \frac{\dot{\phi}^2/2 - V(\phi)}{\dot{\phi}^2/2 + V(\phi)} \quad (9)$$

The EOS has to be very close to -1 during the slow-roll inflation.

(2) The slow-roll parameter ϵ_H , which is defined in terms of H and its derivatives,

$$\epsilon_H = -\frac{\dot{H}}{H^2} \quad (10)$$

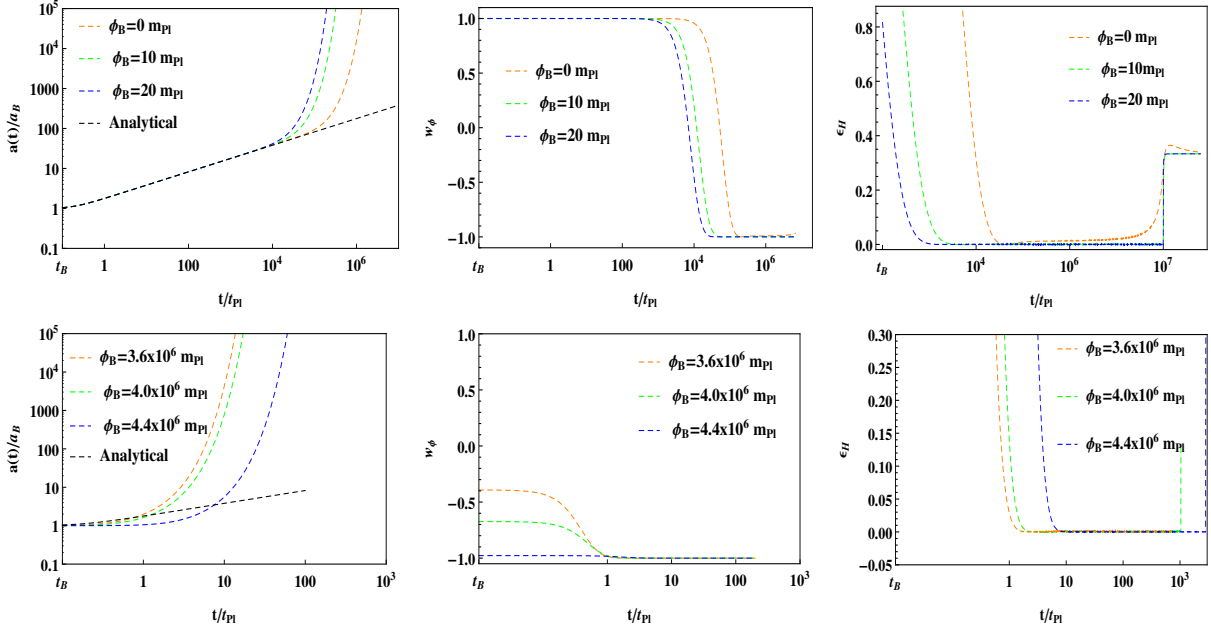


FIG. 1: The numerical solution for the power-law potential with $n = 7/4$ and $\dot{\phi}_B > 0$. The figure shows the evolution of $a(t)$, $w(\phi)$ and ϵ_H for the KED (Top panels) and the PED (Bottom panels) initial conditions at the bounce. In the left panels (Top and Bottom), the analytical solution of $a(t)$ [Eq. (13)] is also exhibited in order to compare it with the numerical results. For the KED case (Top left panel), the evolution of $a(t)$ is universal whereas it is lost in the PED case (Bottom left panel). We use $m = 6.2 \times 10^{-6} m_{pl}$ and $m_{pl} = 1$.

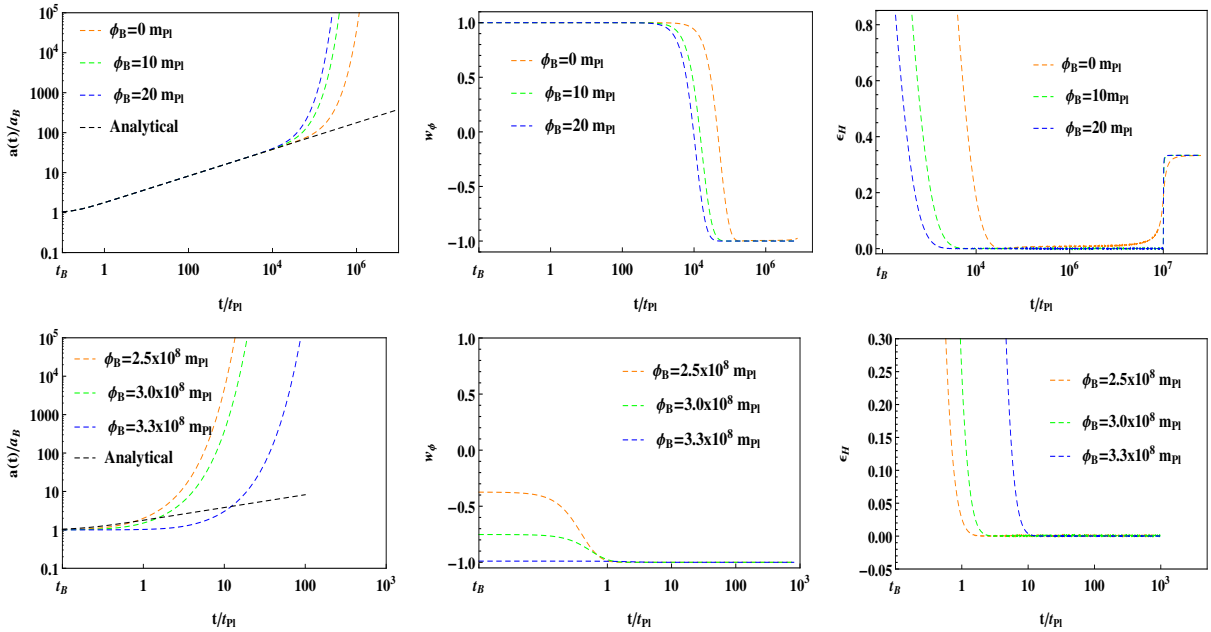


FIG. 2: This figure represents the evolution of $a(t)$, $w(\phi)$ and ϵ_H for the potential with $n = 4/3$ and $\dot{\phi}_B > 0$. Top panels correspond to KED initial conditions whereas the bottom ones are for PED initial conditions. We take $m = 5.1 \times 10^{-5} m_{pl}$ and $m_{pl} = 1$.

During the slow-roll inflation, $\epsilon_H \ll 1$.

(3) The number of e-folds N_{inf} during the slow-roll inflation is defined by

$$\begin{aligned} N_{inf} &= \ln\left(\frac{a_{end}}{a_i}\right) = \int_{t_i}^{t_{end}} H(t) dt \\ &= \int_{\phi_i}^{\phi_{end}} \frac{H}{\dot{\phi}} d\phi \simeq \int_{\phi_{end}}^{\phi_i} \frac{V}{V_{\phi}} d\phi \end{aligned} \quad (11)$$

where a_i represents the time when the universe commences to accelerate i.e. $\ddot{a}(t_i) \gtrsim 0$. The a_{end} is the time when the universe ends to accelerate i.e. $w(\phi_{end}) = -1/3$.

(4) During the bouncing phase, we can obtain an analytical solution of scale factor $a(t)$ by using equations (1) and (3). In the bouncing phase, if the effects of potential are negligible compared to the kinetic energy term then equations (1) and (3) can be written as

$$\begin{aligned} H^2 &= \frac{8\pi}{3m_{pl}^2} \frac{1}{2} \dot{\phi}^2 \left(1 - \frac{\dot{\phi}^2}{2\rho_c}\right), \\ \ddot{\phi} + 3H\dot{\phi} &= 0 \end{aligned} \quad (12)$$

On solving the above equations analytically, we find

$$\begin{aligned} \dot{\phi} &= \pm \sqrt{2\rho_c} \left(\frac{a_B}{a(t)}\right)^3, \\ a(t) &= a_B \left(1 + \delta \frac{t^2}{t_{pl}^2}\right)^{1/6} \end{aligned} \quad (13)$$

where t_{pl} denotes the Planck time, and parameter $\delta = \frac{24\pi\rho_c}{m_{pl}^4}$ represents a dimensionless constant.

(5) We also introduce a new quantity r_w , which is the ratio between the kinetic and potential energies,

$$r_w \equiv \frac{\frac{1}{2}\dot{\phi}^2}{V(\phi)} \quad (14)$$

From which we define r_{cw} as the ratio that corresponds to exactly 60 e-folds during the slow-roll inflation [2],

$$r_{cw} \equiv \left. \frac{\frac{1}{2}\dot{\phi}^2}{V(\phi)} \right|_{N_{inf} \simeq 60} \quad (15)$$

In the following sub-section, we shall discuss power-law potentials with different n in the context of PIV and NIV at the bounce.

A. Positive inflaton velocity: $\dot{\phi}_B > 0$

For power-law potential (4) with $n < 2$, we focus on the positive values of the scalar field ϕ as for negative values of ϕ , potential would be complex (except $n = 1$, in this case, potential would be negative). Therefore, ϕ must be positive in order to keep the potential to be real.

1. Power-law potential with $n = 7/4$

Let us start by considering the evolution equations (1) and (3) with (4) and $n = 7/4$. As mentioned above, we choose only positive values of initial conditions of ϕ_B in order for the potential to be real. Further, it can be divided into two subclasses, KED and PED cases at the bounce.

Fig. 1 (Top panels) corresponds to the KED initial conditions, for which we evolve the equations (1), (3) and (4) numerically, and obtain the evolution of the scale factor $a(t)$, the EOS $w(\phi)$ and the slow-roll parameter ϵ_H for the same set of initial conditions of ϕ_B . It is clearly exhibited that the desired slow-roll inflation for a set of initial conditions is obtained. During this phase, $a(t)$ is exponentially increasing (Top left panel of Fig. 1), $w(\phi)$ is nearly close to -1 (Top middle panel of Fig. 1), and $\epsilon_H \ll 1$ (Top right panel of Fig. 1).

From the top middle panel of Fig. 1, we notice that the evolution of the universe can be split into three phases, namely bouncing, transition and the slow-roll [8]. In the bouncing phase, the kinetic energy is dominated, and $w(\phi) \simeq +1$. In the transition phase ($t/t_{pl} \simeq 10^4$), $w(\phi)$ changes from $+1$ to -1 ($t/t_{pl} \simeq 10^5$). In the slow-roll phase, $w(\phi)$ remains to -1 till the end of the slow-roll inflation. In the bouncing phase, it is astounding to note that the evolution of $a(t)$ is independent for a wide varieties of initial conditions of ϕ_B , and can be well approximated by the analytical solution (13).

Next, we calculate the number of e-folds N_{inf} during the slow-roll inflation for any choice of ϕ_B in the range $(0, \phi_{max})$, and the relevant quantities are shown in Table I. For the successful inflation, at least 60 e-folds are needed and to get it, one has to require

$$\phi_B \in (0.805m_{pl}, \phi_{max}) \quad (16)$$

where

$$\phi_{max} = \left(\frac{16\rho_c^4}{m^9}\right)^{1/7} \equiv 4.4284 \times 10^6 \quad (17)$$

From Table I, we can clearly see that N_{inf} increases as ϕ_B increases, this implies that the larger values of ϕ_B give rise to more number of e-folds during the slow-roll inflation. The similar results for power-law potential with $n = 2$ are shown in [8].

The bottom panels of Fig. 1 are shown for the PED initial conditions at the bounce. In this case, one can clearly notice that the universality of the scale factor $a(t)$ is lost, and the bouncing phase does not exist any more, though the slow-roll inflationary phase $w(\phi) \simeq -1$ can still be obtained. As mentioned above, we get more number of e-folds for the larger values of ϕ_B , as Table I shows.

2. Power-law potential with $n = 4/3$

In this sub-section, we consider power-law potential with $n = 4/3$. Similar to the case of $n = 7/4$, we choose

TABLE I: Table for the number of e-foldings N_{inf} , $r_{cw}(N_{inf} \simeq 60)$ and $r_w(60 < N_{inf} < 60)$ with $\dot{\phi}_B > 0$. The values of ϕ_B start from the KED case and approach till the end of PED one. In PED initial conditions, we put the sign of \simeq as both values of ϕ_* are not exactly equal.

n	m	ϕ_B	Inflation	t/t_{pl}	ϕ_*	N_{inf}	r_{cw}/r_w
7/4	6.2×10^{-6}	0	starts	6.6745×10^4	2.18488	38.5781	$r_{cw} > r_w$
			ends	1.111×10^7	0.180914		
		0.5	starts	5.6425×10^4	2.65752	53.7887	$r_{cw} > r_w$
			ends	1.309×10^7	0.267712		
		0.795	starts	5.17513×10^4	2.93845	57.7869	$r_{cw} > r_w$
			ends	1.0699×10^7	1.34347		
		0.805	starts	5.16106×10^4	2.948	60.3252	$r_{cw} = r_w$
			ends	1.2024×10^7	1.5552		
		1.0	starts	4.8950×10^4	3.13439	63.7207	$r_{cw} < r_w$
			ends	1.119×10^7	1.67068		
3.0	starts	3.23156×10^4	5.06678	105.443	$r_{cw} < r_w$		
	ends	1.0402×10^7	3.74002				
(PED)	4×10^6	starts	0.577	$\simeq 4 \times 10^6$	714.0459	$r_{cw} < r_w$	
		ends	1047.32	$\simeq 4 \times 10^6$			
4/3	5.1×10^{-5}	0	starts	5.81699×10^4	2.16248	50.4897	$r_{cw} > r_w$
			ends	1.16825×10^7	0.11362		
		0.35	starts	5.29494×10^4	2.49717	57.8107	$r_{cw} > r_w$
			ends	1.02966×10^7	0.937812		
		0.4005	starts	5.22858×10^4	2.54562	60.0079	$r_{cw} = r_w$
			ends	1.0607×10^7	1.04617		
		0.5	starts	5.10331×10^4	2.64118	62.4811	$r_{cw} < r_w$
			ends	1.06214×10^7	0.856514		
		1.0	starts	4.57248×10^4	3.12329	71.8501	$r_{cw} < r_w$
			ends	1.01714×10^7	1.76734		
3.0	starts	3.32295×10^4	5.07132	107.173	$r_{cw} < r_w$		
	ends	1.00928×10^7	4.00218				
(PED)	2.5×10^8	starts	0.401	$\simeq 2.5 \times 10^8$	710.9396	$r_{cw} < r_w$	
		ends	827.735	$\simeq 2.5 \times 10^8$			
(PED)	3.0×10^8	starts	0.665	$\simeq 3.0 \times 10^8$	714.4861	$r_{cw} < r_w$	
		ends	1.17643×10^3	$\simeq 3.0 \times 10^8$			

TABLE II: Table for N_{inf} , $r_{cw}(N_{inf} \simeq 60)$ and $r_w(60 < N_{inf} < 60)$ with $\dot{\phi}_B > 0$.

n	m	ϕ_B	Inflation	t/t_{pl}	ϕ_*	N_{inf}	r_{cw}/r_w
1	1.9×10^{-4}	0	starts	4.82718×10^4	2.13211	63.6793	$r_{cw} < r_w$
			ends	1.04513×10^7	0.152698		
		0.01	starts	4.8161×10^4	2.14174	64.7404	$r_{cw} < r_w$
			ends	1.07438×10^7	0.075339		
		0.05	starts	4.774×10^4	2.18031	66.0862	$r_{cw} < r_w$
			ends	1.06922×10^7	0.169875		
0.1	starts	4.72339×10^4	2.22857	69.9625	$r_{cw} < r_w$		
	ends	1.18715×10^7	0.574322				
0.5	starts	4.36669×10^4	2.61579	78.0678	$r_{cw} < r_w$		
	ends	1.0538×10^7	0.929275				
2/3	4.7×10^{-4}	(PED) 1.0×10^{11}	starts	0.575	$\simeq 1.0 \times 10^{11}$	714.3224	$r_{cw} < r_w$
			ends	1.0474×10^3	$\simeq 1.0 \times 10^{11}$		
		0	starts	5.05957×10^4	2.13979	72.75	$r_{cw} < r_w$
			ends	1.06725×10^7	0.843284		
		0.01	starts	5.05283×10^4	2.14957	73.1079	$r_{cw} < r_w$
			ends	1.07272×10^7	1.44494		
0.1	starts	4.9876×10^4	2.23745	74.2893	$r_{cw} < r_w$		
	ends	1.0638×10^7	0.998999				
1.0	starts	4.47227×10^4	3.11971	85.8929	$r_{cw} < r_w$		
	ends	1.06634×10^7	2.79913				
(PED) 1.5×10^{16}	starts	0.343	$\simeq 1.5 \times 10^{16}$	715.7368	$r_{cw} < r_w$		
	ends	796.18	$\simeq 1.5 \times 10^{16}$				
(PED) 3.0×10^{16}	starts	1.06	$\simeq 3.0 \times 10^{16}$	716.2100	$r_{cw} < r_w$		
	ends	1805.14	$\simeq 3.0 \times 10^{16}$				
1/3	1.1×10^{-3}	0	starts	4.35782×10^4	2.11548	86.5305	$r_{cw} < r_w$
			ends	1.00983×10^7	1.57308		
		0.01	starts	4.36×10^4	2.12553	88.5284	$r_{cw} < r_w$
			ends	1.03913×10^7	1.40504		
		2.0	starts	3.92×10^4	4.09819	97.6823	$r_{cw} < r_w$
			ends	1.00755×10^7	3.8348		
(PED) 3.0×10^{31}	starts	0.3109	$\simeq 3.0 \times 10^{31}$	715.3383	$r_{cw} < r_w$		
	ends	781.16	$\simeq 3.0 \times 10^{31}$				

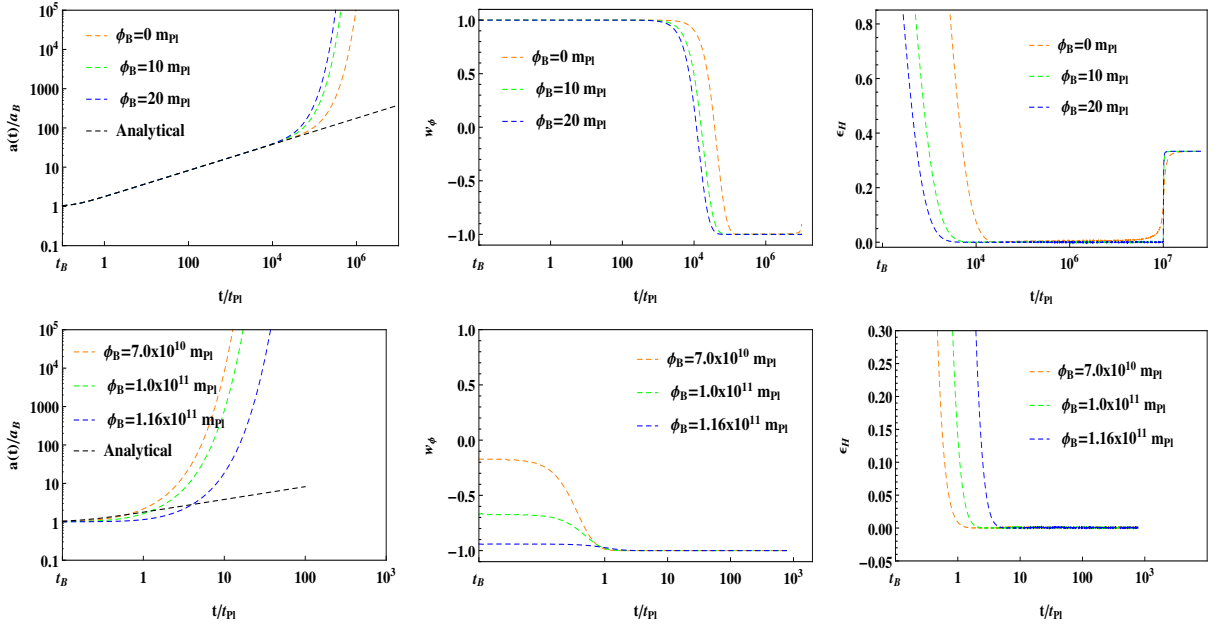


FIG. 3: This figure is displayed for $n = 1$ and $\dot{\phi}_B > 0$. We choose $m = 1.9 \times 10^{-4} m_{pl}$ and $m_{pl} = 1$.

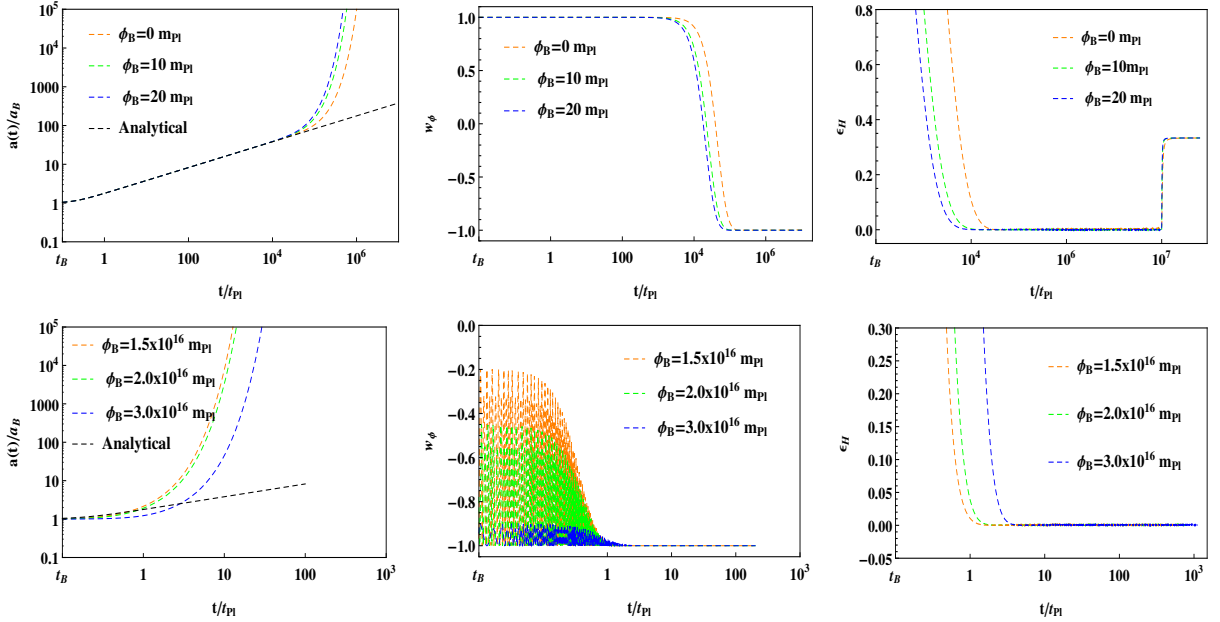


FIG. 4: This figure exhibits the numerical evolution of $a(t)$, $w(\phi)$ and ϵ_H with $n = 2/3$ and $\dot{\phi}_B > 0$ for the different sets of initial conditions. We consider $m = 4.7 \times 10^{-4} m_{pl}$ and $m_{pl} = 1$.

only positive values of the scalar field to get the real potential. Later, the initial conditions at the quantum bounce can be divided into two categories such as KED and PED initial conditions.

Let us first focus on the case in which the evolution at the quantum bounce is dominated by the kinetic energy of the inflaton field. To this effect, we numerically evolve

the system (1) and (3) with (4) and $n = 4/3$. The results are shown in the top panels of Fig. 2. The evolution of analytical solution of $a(t)$ (13) is also illustrated to compare it with the numerical solutions, and found to be universal (Top left panel of Fig. 2).

As we discussed in the case of $n = 7/4$, here also the evolution of the universe is divided into three phases;

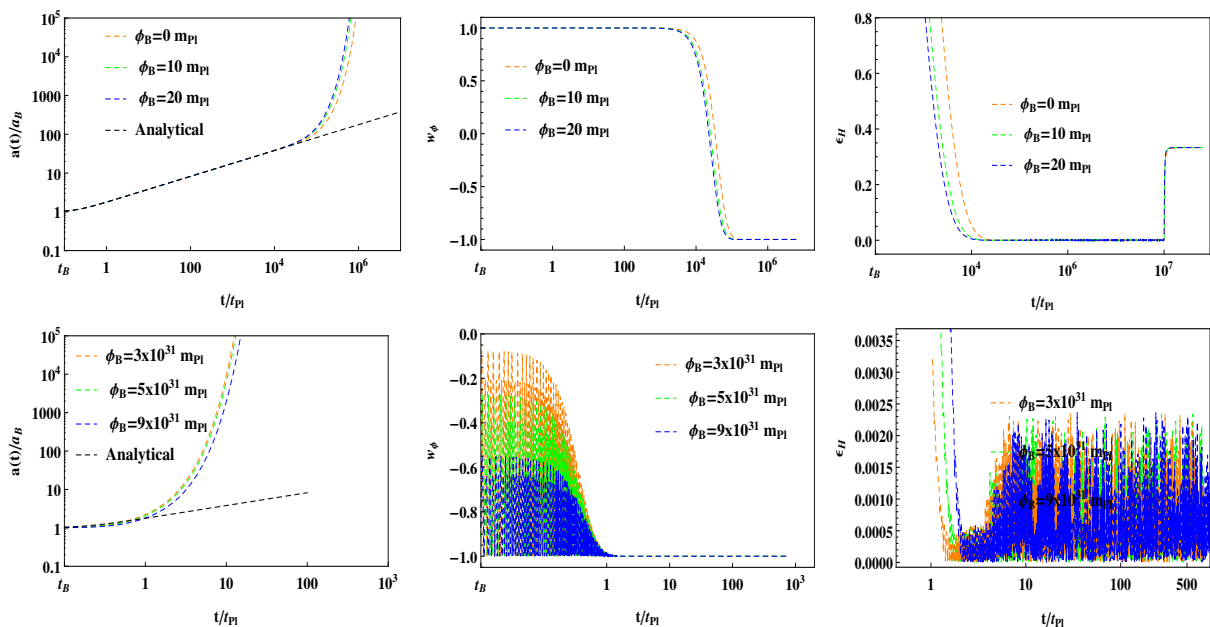


FIG. 5: This figure is plotted for $n = 1/3$ and $\dot{\phi}_B > 0$. Here, $m = 1.1 \times 10^{-3} m_{pl}$ and $m_{pl} = 1$.

bouncing, transition, and the slow-roll (Top middle panel of Fig. 2). In the bouncing phase, the evolution of $a(t)$ is independent not only on the different kind of initial values of ϕ_B but also the inflationary potential. This is mainly due to the small amplitude of the potential in comparing with the kinetic term, and its effects on the evolution during the bouncing phase is almost insignificant.

Top right panel of Fig. 2 demonstrates the evolution of the slow-roll parameter ϵ_H . The slow-roll inflation regime can be obtained for any choices of ϕ_B in the range $(0, \phi_{max})$ (see Table I). However, in order to get at least 60 e-folds during the slow-roll regime, the values of ϕ_B should be in the following range

$$\phi_B \in (0.4005 m_{pl}, \phi_{max}) \quad (18)$$

where

$$\phi_{max} = \left(\frac{8\rho_c^3}{m^8} \right)^{1/4} \equiv 3.31299 \times 10^8 \quad (19)$$

Bottom panels of Fig. 2 represent the evolution of $a(t)$, $w(\phi)$ and ϵ_H for the PED initial conditions at the bounce. In this case, the bouncing phase no longer exists and the universality of the scale factor disappears. However, slow-roll inflationary phase can still be achieved. Similar to the case of $n = 7/4$, as ϕ_B increases we get more and more number of e-folds. In other words, the PED initial conditions can produce a large number of e-folds N_{inf} during the slow-roll inflationary phase (see Table I).

3. Power-law potential with $n = 1, 2/3$ and $1/3$

In this sub-section, we shall study the cases $n = 1, 2/3$ and $1/3$ for the power-law potential. Similar to the sub-sections II A 1 and II A 2, for all the three cases, ϕ_B must be positive to obtain the real potential. Further the initial conditions at the quantum bounce can be divided into two categories, namely KED and PED.

Let us first consider the KED case at the bounce. We numerically solve the equations (1) and (3) with (4) and $n = 1, 2/3$ and $1/3$, respectively. The results are displayed in the top panels of Figs. 3, 4 and 5, respectively. In the top left panels, the evolution of $a(t)$ at the bounce are independent of the different sets of initial conditions and represent a universal feature. We also depict the analytical solution of $a(t)$ (13) in comparison to the numerical solutions. As mentioned in sub-sections II A 1 and II A 2, here also the evolution of the universe for $n = 1, 2/3$ and $1/3$ can be split into three regimes: bouncing, transition and the slow-roll. The corresponding number of e-folds N_{inf} for each case are shown in Table II.

For these cases, the desired slow-roll inflation is achieved for any values of ϕ_B in the range $(0, \phi_{max})$. In the said range, we also have more than 60 e-folds in contrast to the cases of $n = 7/4$ and $4/3$ where to obtain at least 60 e-folds the ranges were restricted.

For the different cases of n , the ϕ_{max} are found to be:

For $n = 1$,

$$\phi_{max} = \frac{2\rho_c}{m^3} \simeq 1.19551 \times 10^{11} \quad (20)$$

for $n = 2/3$,

$$\phi_{max} = \left(\frac{8\rho_c^3}{m^{10}} \right)^{1/2} \simeq 3.23766 \times 10^{16} \quad (21)$$

and for $n = 1/3$,

$$\phi_{max} = \frac{8\rho_c^3}{m^{11}} \simeq 1.1932511 \times 10^{32} \quad (22)$$

Finally, in the above cases, we consider the PED initial conditions at the bounce. The numerical results are illustrated in the bottom panels of Figs. 3, 4 and 5, respectively. In each case, the evolution of $a(t)$ at the bounce is very sensitive to the set of initial conditions, and the universal features of it disappear. Specifically, the bouncing phase no longer exists. Although, the slow-roll regime $w(\phi) \simeq -1$ can still be achieved, see bottom panels of Figs. 3, 4 and 5. Additionally, the PED initial conditions can lead to a large number of e-folds N_{inf} during the slow-roll inflationary regime that are shown in Table II.

B. Negative inflaton velocity: $\dot{\phi}_B < 0$

To cover the entire phase space we should also study the NIV at the bounce ($\dot{\phi}_B < 0$). Similar to the previous sub-sections, in this sub-section, we choose the positive values of inflaton field at the bounce ($\phi_B > 0$) in order to keep the potential to be real. The detailed investigations for the power-law potential with $n < 2$ are given below.

1. Power-law potential with $n = 7/4$

Numerically, we evolve the system (1) and (3) with (4) and $n = 7/4$. Again, we have two cases such as KED and PED at the quantum bounce.

First we discuss the KED one, in which, top panels of Fig. 6 show the evolution of $a(t)$, $w(\phi)$ and ϵ_H for a set of initial values of ϕ_B . In the top left panel, we also exhibit the analytical solution of $a(t)$ (13) in comparison to the numerical solutions. Furthermore, we have three regimes; bouncing, transition and the slow-roll (Top middle panel of Fig. 6). Next, we calculate the number of e-folds N_{inf} during the slow-roll regime for the restricted range of ϕ_B , and given by (see Table III)

$$\phi_B \in (4.3m_{pl}, \phi_{max}) \quad (23)$$

where ϕ_{max} is given by Eq. (17). Note that we do not obtain the slow-roll regime with $\phi_B = 0, 0.5, 1$ and 2 etc. for ($\dot{\phi}_B < 0$). However, in sub-section II A 1, for the positive inflaton velocity ($\dot{\phi}_B > 0$), the slow-roll regime covers the whole range of ϕ_B as $\phi_B \in (0, \phi_{max})$. To get at least 60 e-folds during the slow-roll inflation, ϕ_B has to be restricted as shown in Table III:

$$\phi_B \in (5.3m_{pl}, \phi_{max}) \quad (24)$$

For the PED conditions, the evolution of $a(t)$, $w(\phi)$ and ϵ_H are shown in the bottom panels of Fig. 6 for different initial values of ϕ_B . In this case, the universality of $a(t)$ has been lost and the bouncing phase does not exist any more. Though inflationary regime can be achieved. As ϕ_B grows, we get more number of e-folds, see Table III.

2. Power-law potential with $n = 4/3, 1, 2/3$ and $1/3$

Figs. 7, 8, 9 and 10 are plotted for $n = 4/3, 1, 2/3$ and $1/3$, respectively, and show the evolutions of $a(t)$, $w(\phi)$ and ϵ_H for different sets of initial values of ϕ_B . Top panels correspond to the KED case whereas bottom ones are for PED conditions. For each value of n , we get desired slow-roll inflationary phase. To obtain at least 60 e-folds during the slow-roll regime each n has restricted range given as follows.

For $n = 4/3$,

$$\phi_B \in (4.889m_{pl}, \phi_{max}) \quad (25)$$

for $n = 1$,

$$\phi_B \in (4.41m_{pl}, \phi_{max}) \quad (26)$$

for $n = 2/3$,

$$\phi_B \in (4.02m_{pl}, \phi_{max}) \quad (27)$$

and for $n = 1/3$,

$$\phi_B \in (3.49m_{pl}, \phi_{max}) \quad (28)$$

where ϕ_{max} for $n = 4/3, 1, 2/3$ and $1/3$ are given by the equations (19), (20), (21) and (22), respectively.

The PED initial conditions lead to a large number of e-folds during the slow roll regime, and are shown in Tables III and IV.

III. PHASE PORTRAIT AND THE DESIRED SLOW-ROLL INFLATION

According to Planck 2015 results [2], the power-law potential with $n = 2$ is moderately disfavored compared to the models predicting a smaller tensor-to-scalar ratio, such as R^2 inflationary model proposed by Starobinsky [42]. However, the power-law potential with $n < 2$ is consistent with the Planck 2015 results. Therefore, in this section, we shall study the phase space analysis for the power-law potentials with $n = 7/4, 4/3, 1, 2/3$ and $1/3$, respectively. The detailed analysis are given below.

As we mentioned in section II A, the inflaton field ϕ must be positive, to get the real potential. Conclusively, it would cover only the half phase space (semi-circle). To obtain the whole phase space, more precisely, to show the phase space trajectories in a complete circle,

TABLE III: Table for N_{inf} , $r_{cw}(N_{inf} \simeq 60)$ and $r_w(60 < N_{inf} < 60)$ with $\dot{\phi}_B < 0$.

n	m	ϕ_B	Inflation	t/t_{pl}	ϕ_*	N_{inf}	r_{cw}/r_w
7/4	6.2×10^{-6}	4.3	starts	7.18583×10^4	2.10286	29.4384	$r_{cw} > r_w$
			ends	9.531×10^6	0.169577		
		5	starts	5.48084×10^4	2.84702	52.3782	$r_{cw} > r_w$
			ends	1.2252×10^7	0.378438		
5.3	starts	4.99183×10^4	3.16226	60.6001	$r_{cw} = r_w$		
	ends	1.225×10^7	0.632925				
6.0	starts	4.15123×10^4	3.89232	75.6016	$r_{cw} < r_w$		
	ends	1.0707×10^7	2.25377				
(PED)	4×10^6	4.81	starts	0.577	$\simeq 3.9 \times 10^6$	713.8254	$r_{cw} < r_w$
			ends	1046.48	$\simeq 3.9 \times 10^6$		
4/3	5.1×10^{-5}	4.81	starts	5.19777×10^4	2.66568	57.2321	$r_{cw} > r_w$
			ends	1.0493×10^7	0.6593		
		4.889	starts	5.09254×10^4	2.74802	60.1178	$r_{cw} = r_w$
			ends	1.0757×10^7	0.678072		
5.0	starts	4.95217×10^4	2.86358	62.1697	$r_{cw} < r_w$		
	ends	1.0444×10^7	1.18179				
6.0	starts	4.0199×10^4	3.89758	84.6534	$r_{cw} < r_w$		
	ends	1.044×10^7	2.55716				
(PED)	3×10^8	4.81	starts	0.665	$\simeq 3.0 \times 10^8$	714.7624	$r_{cw} < r_w$
			ends	1178.2	$\simeq 3.0 \times 10^8$		
1	1.9×10^{-4}	4.34	starts	4.85251×10^4	2.2069	56.5358	$r_{cw} > r_w$
			ends	9.704×10^6	0.0783571		
		4.41	starts	4.77327×10^4	2.27959	60.4555	$r_{cw} = r_w$
			ends	1.02023×10^7	0.0781092		
4.45	starts	4.72885×10^4	2.32111	62.7961	$r_{cw} < r_w$		
	ends	1.0493×10^7	0.0772239				
5.0	starts	4.23001×10^4	2.88928	80.3628	$r_{cw} < r_w$		
	ends	1.0803×10^7	0.889376				
(PED)	1.0×10^{11}	4.34	starts	0.575	$\simeq 1.0 \times 10^{11}$	714.4728	$r_{cw} < r_w$
			ends	1048.3	$\simeq 1.0 \times 10^{11}$		

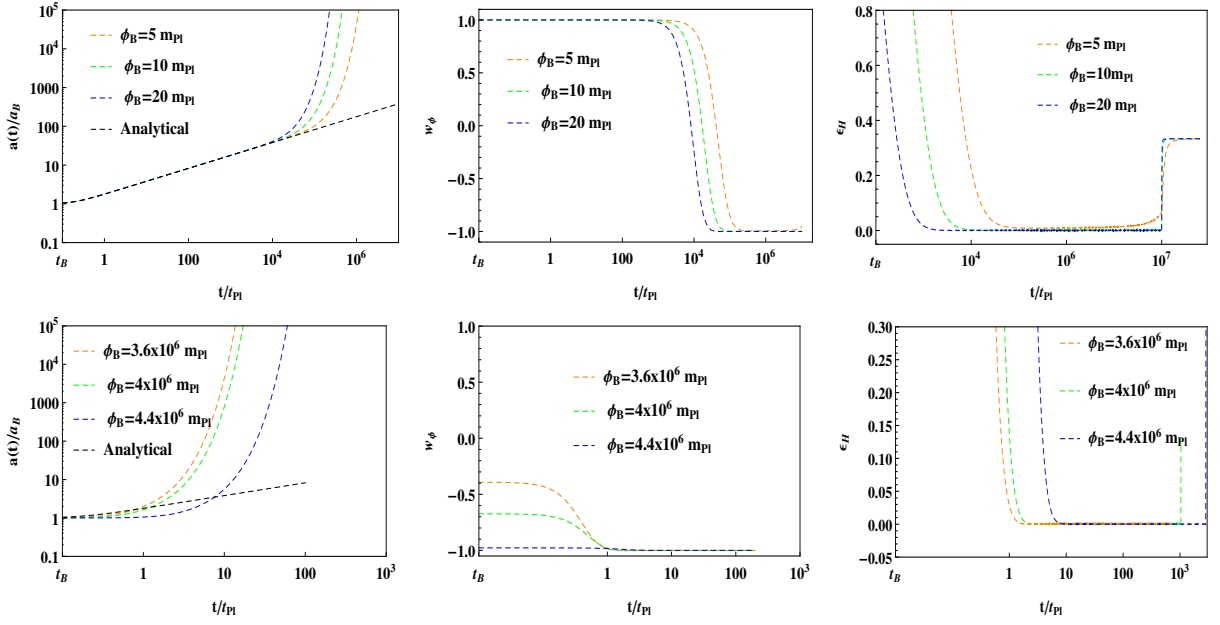


FIG. 6: This figure shows the numerical evolution of $a(t)$, $w(\phi)$ and ϵ_H for the potential with $n = 7/4$ and $\dot{\phi}_B < 0$. Top panels demonstrate the evolution for KED initial conditions whereas bottom ones are for PED.

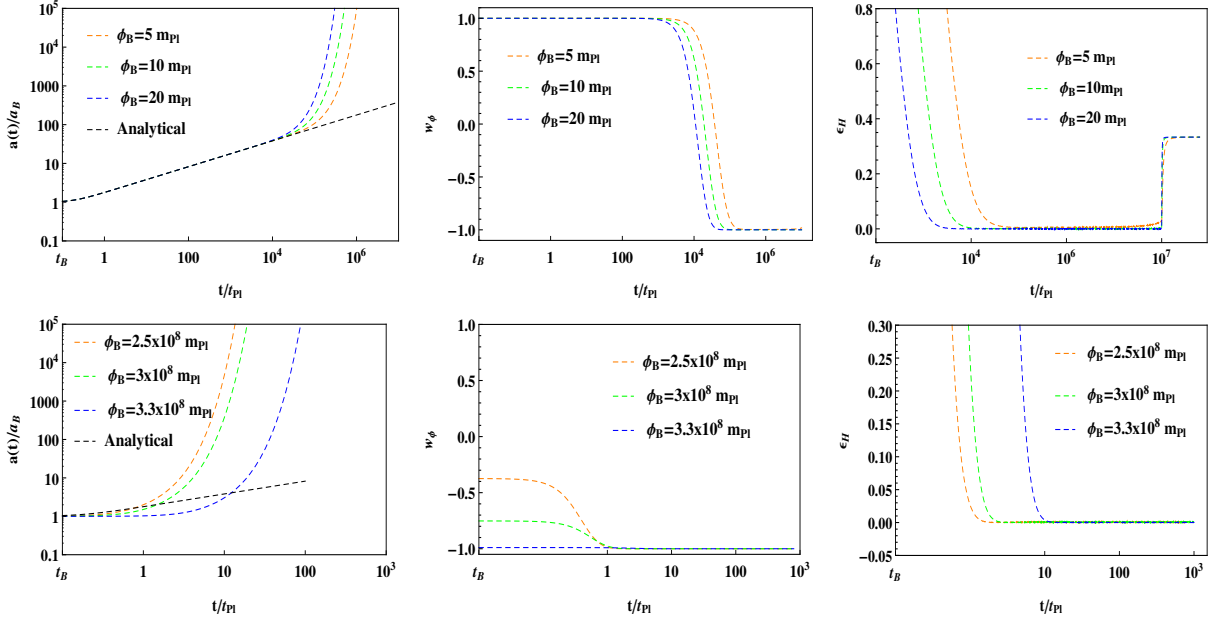


FIG. 7: This figure represents the numerical solutions for the potential with $n = 4/3$ and $\dot{\phi}_B < 0$.

we introduce the following dimensionless quantities

$$\xi = \pm \sqrt{\frac{V(\phi)}{\rho_c}}, \quad y = \pm \frac{\dot{\phi}}{\sqrt{2\rho_c}}, \quad \tau = mt \quad (29)$$

to form an autonomous system of evolution equations,

which are given by

$$\begin{aligned} \frac{d\xi}{d\tau} &= \pm \sqrt{2V_0} \frac{n}{2m} \left(\frac{\rho_c \xi^2}{V_0} \right)^{\frac{n-2}{2n}} y \\ \frac{dy}{d\tau} &= -3Hy/m - \frac{V_0 n}{m\sqrt{2\rho_c}} \left(\frac{\rho_c \xi^2}{V_0} \right)^{\frac{n-1}{n}} \end{aligned} \quad (30)$$

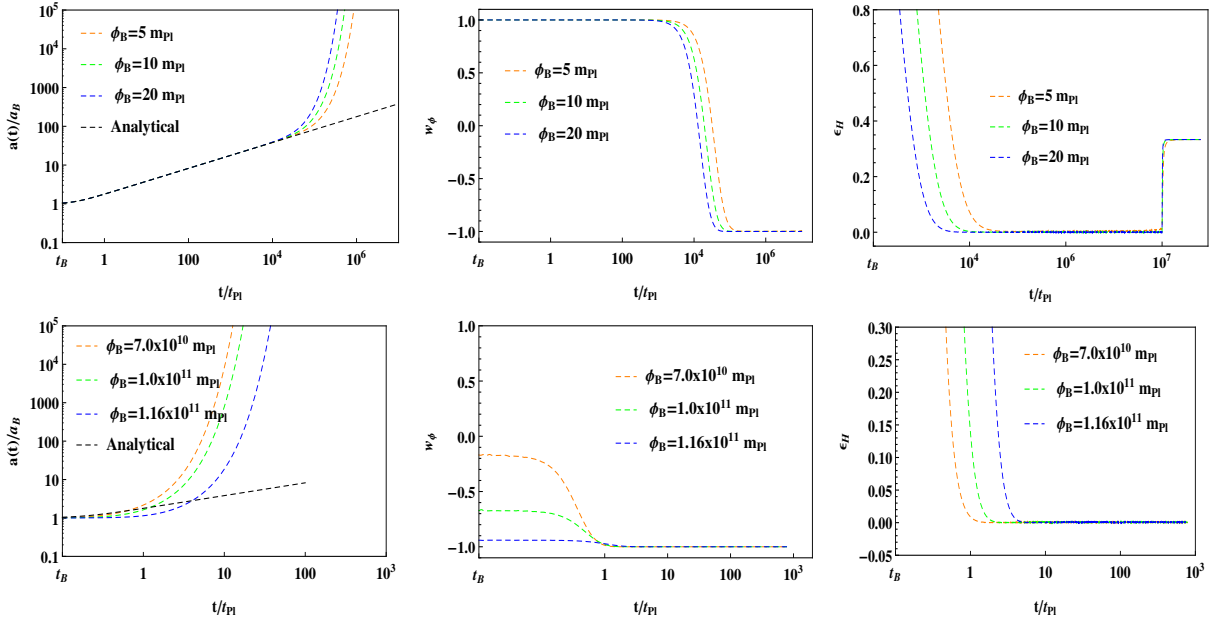


FIG. 8: This figure is for $n = 1$ and $\dot{\phi}_B < 0$.

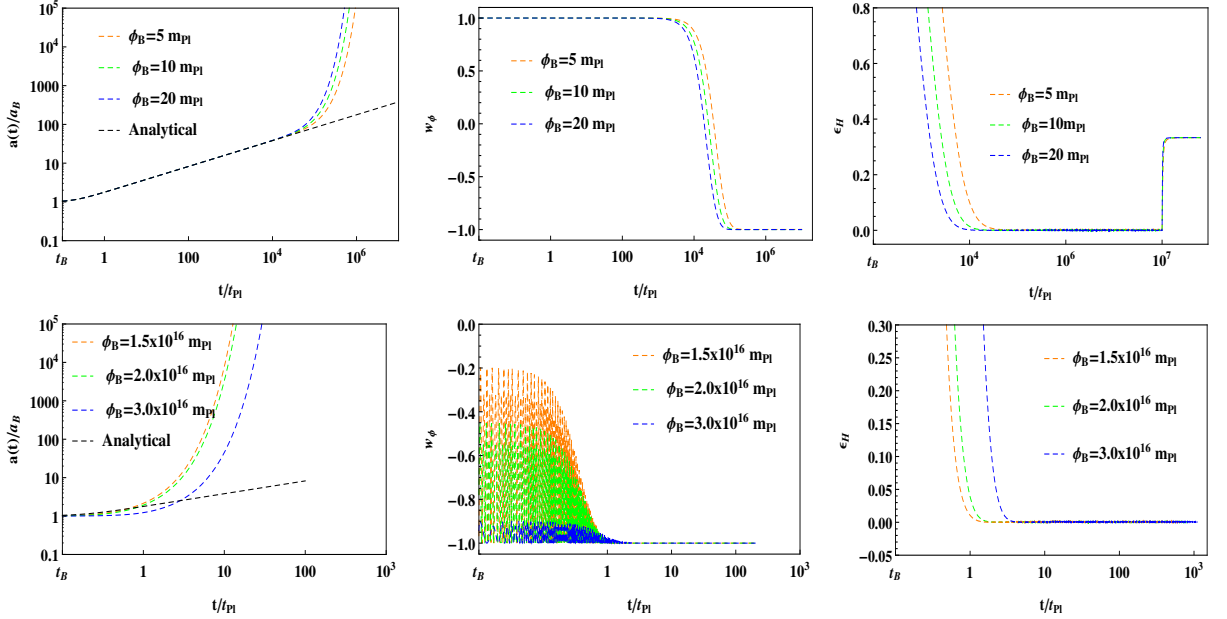


FIG. 9: This figure corresponds to $n = 2/3$ and $\dot{\phi}_B < 0$.

where $V(\phi) = V_0\phi^n$, and $V_0 = 1/2 m^{4-n}$. At the bounce, we have $\rho = \rho_c$, this implies that

$$\xi_B^2 + y_B^2 = 1 \quad (31)$$

This is the equation of a circle. Thus, for the chosen dimensionless variables, we obtain equation of the circle at the quantum bounce irrespective of n .

First we do analysis for $n = 7/4$. Tables I and III

are obtained for PIV ($\dot{\phi}_B > 0$) and NIV ($\dot{\phi}_B < 0$). By looking at both tables, we observe that the observationally compatible initial conditions are $\phi_B \geq 0.805m_{pl}$ for $\dot{\phi}_B > 0$ and $\phi_B \geq 5.3m_{pl}$ for $\dot{\phi}_B < 0$. Therefore, in the whole parameter space of initial conditions these are only the KED initial conditions which can produce the desired slow-roll inflationary regime in their future evolution. However, some of the KED initial conditions do

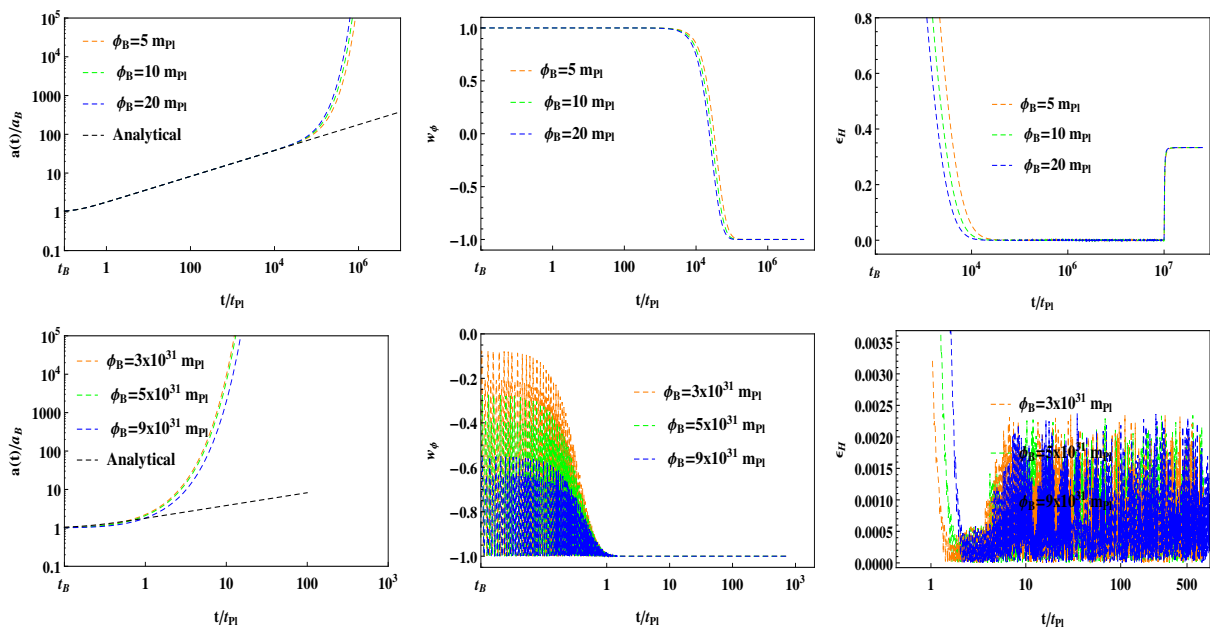


FIG. 10: The numerical evolutions are displayed for $n = 1/3$ and $\dot{\phi}_B < 0$

not provide the desired slow-roll, see the values of ϕ_B in Tables I and III. All the PED initial conditions at the bounce can lead to the desired slow-roll phase, and a large number of e-folds can be obtained, as shown in Tables I and III.

Top panel of Fig. 11 shows the evolution of the phase space trajectories for both PIV and NIV, and also for both the KED and PED initial conditions, more accurately, it corresponds to the entire phase space. Regions close to the boundary of the circle represent the large energy density with the dominance of the quantum effects whereas small energy limit exists near the origin in the $\xi - y$ plane. All the phase space trajectories are started from the bounce ($\rho = \rho_c$), and directed towards the origin which is the only stable point. The main characteristic of these portraits is the inflationary separatrix [17] that is shown in the figure where all the trajectories are attracted towards the origin.

Second, we consider the power-law potential with $n = 4/3$. In this case, we obtain 60 or more e-folds at the initial conditions $\phi_B \geq 0.4005m_{pl}$ for $\dot{\phi}_B > 0$ and $\phi_B \geq 4.889m_{pl}$ for $\dot{\phi}_B < 0$. Similar to the case of $n = 7/4$, here also some KED initial conditions do not provide the desired slow-roll phase. In the case of PED initial conditions, the enormous amount of inflation is obtained, see Tables I and III. The phase portrait for this case is exhibited in the middle panel of Fig. 11.

Third, we study the potential with $n = 1$. For PIV ($\dot{\phi}_B > 0$), the whole range of KED initial conditions of ϕ_B ($\phi_B \geq 0$) is consistent with the observations whereas in case of NIV ($\dot{\phi}_B < 0$), it should be restricted as $\phi_B \geq 4.41m_{pl}$. This implies that, in the case of $\dot{\phi}_B > 0$,

the entire range of KED initial conditions ($\phi_B \geq 0$) can produce the desired slow-roll phase, and lead to more than 60 e-folds which do not possible in the cases of $n = 7/4$ and $4/3$. All the PED initial conditions can give rise to a large amount of inflation, see Tables II and III. The corresponding phase portrait is shown in the bottom panel of Fig. 11.

Next, we focus on the potential with $n = 2/3$. Here also, for $\dot{\phi}_B > 0$, the entire range of ϕ_B ($\phi_B \geq 0$) is in a good agreement with the observations whereas for $\dot{\phi}_B < 0$, it is restricted $\phi_B \geq 4.02m_{pl}$ that is shown in Tables II and IV. Top panel of Fig. 12 demonstrates the phase space trajectories for the case under consideration.

Finally, we deal with the potential $n = 1/3$. In this case, the observationally compatible KED initial conditions are $\phi_B \geq 0$ for $\dot{\phi}_B > 0$ and $\phi_B \geq 3.49m_{pl}$ for $\dot{\phi}_B < 0$. The PED initial conditions provide a large number of e-folds, see Tables II and IV. The phase portrait in this case is shown in the bottom panel of Fig. 12.

We are now in position to compare our results with the consequences that are studied in the literature for the quadratic and Starobinsky potentials [8, 19, 23]. Our studies for the power-law potentials with $n < 2$ are in compatible with the quadratic potential. However, quadratic potential has been almost ruled out by the Planck data [2]. In terms of number of e-folds, both KED and PED initial conditions are in good agreement with observations for the potentials with $n < 2$ while Starobinsky inflation is observationally consistent only for KED initial conditions and not for PED ones at the bounce [8, 23].

TABLE IV: Table represents the number of e-foldings N_{inf} , $r_{cw}(N_{inf} \simeq 60)$ and $r_w(60 < N_{inf} < 60)$ with $\dot{\phi}_B < 0$.

n	m	ϕ_B	Inflation	t/t_{pl}	ϕ_*	N_{inf}	r_{cw}/r_w
2/3	4.7×10^{-4}	3.0	starts	7.21753×10^4	0.802212	10.0481	$r_{cw} > r_w$
			ends	2.372×10^6	0.0418586		
		4.0	starts	5.40072×10^4	1.84949	58.4348	$r_{cw} > r_w$
			ends	1.0068×10^7	0.0428617		
		4.02	starts	5.37956×10^4	1.87013	60.0514	$r_{cw} = r_w$
ends	1.0349×10^7	0.00925105					
4.2	starts	5.20966×10^4	2.05536	67.2913	$r_{cw} < r_w$		
ends	1.0875×10^7	0.849753					
1/3	1.1×10^{-3}	3.0	starts	5.13333×10^4	0.857781	22.3829	$r_{cw} > r_w$
			ends	3.368×10^6	0.0115291		
		3.49	starts	4.73607×10^4	1.3609	60.5475	$r_{cw} = r_w$
			ends	8.3017×10^6	0.0114196		
		4.0	starts	4.4815×10^4	1.87991	82.7795	$r_{cw} < r_w$
ends	1.0211×10^7	0.872017					
5.0	starts	4.16413×10^4	2.89187	93.8514	$r_{cw} < r_w$		
ends	1.067×10^7	2.71606					
		(PED) 3.0×10^{16}	starts	1.06	$\simeq 3.0 \times 10^{16}$	716.1492	$r_{cw} < r_w$
			ends	1805.14	$\simeq 3.0 \times 10^{16}$		
		(PED) 3.0×10^{31}	starts	0.3109	$\simeq 3.0 \times 10^{31}$	715.3383	$r_{cw} < r_w$
			ends	781.16	$\simeq 3.0 \times 10^{31}$		

IV. CONCLUSIONS

In the framework of LQC, we studied the pre-inflationary dynamics of the power-law potential with $n < 2$ for PIV and NIV, and also for KED and PED cases. We restricted ourselves to the said potential as the quadratic potential has been moderately disfavored by the Planck 2015 data [2]. In addition, we chose only positive values of inflaton field in order to keep the potential to be real. First, we considered PIV at the quantum bounce, the evolution of background is divided into KED and PED cases. In case of KED initial conditions, the

universe is always split into three different phases prior to the preheating, *bouncing*, *transition* and the *slow-roll*. In the bouncing phase, the background evolution is independent not only on the wide varieties of initial conditions but also the potentials. Specifically, the numerical evolution of the scale factor has shown the universal feature and compared by the analytical solution (13), see upper panels of Figs. 1–5. During this phase, the EOS remains practically $w(\phi) \simeq 1$. However, in transition phase, it decreases rapidly from $w(\phi) \simeq 1$ to $w(\phi) \simeq -1$. The period of the transition regime is very short in comparison with other two regimes. Thereafter, the universe

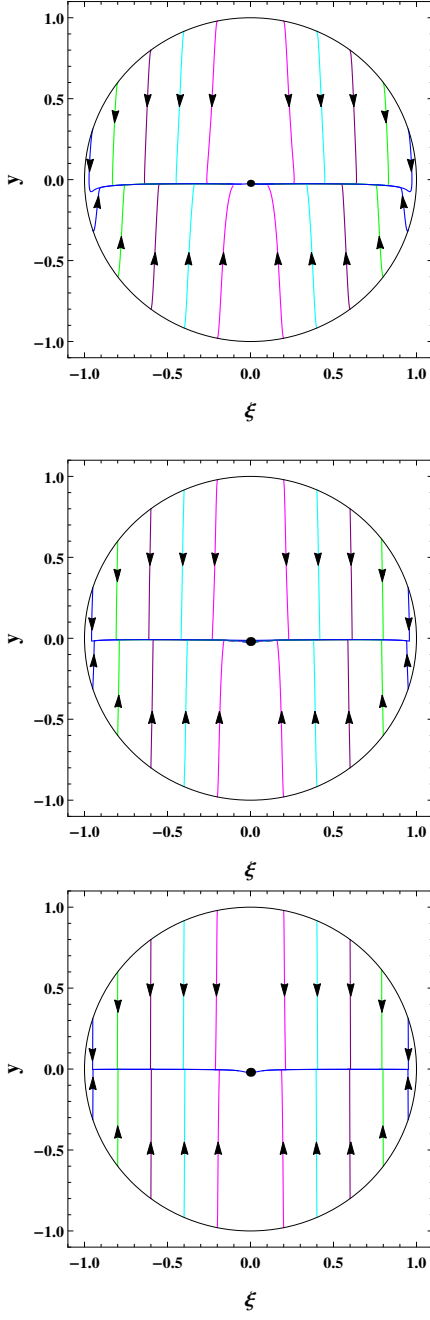


FIG. 11: This figure shows the evolution of phase space trajectories for the power-law potential with $n = 7/4$ (Top), $4/3$ (Middle) and 1 (Bottom). The arrows represent the direction of the trajectories from boundary to the origin. For the better depiction, we choose $m = 0.2m_{pl}$.

enters into an accelerating regime, where the slow-roll parameter ϵ_H is still large, later it drastically decreases to almost zero, by which the slow-roll inflation commences, as shown in upper panels of Figs. 1–5. Next, we calculated the number of e-folds N_{inf} during the slow-roll inflation, and presented in Tables I and II. In case of PED initial conditions, the universality of expansion fac-

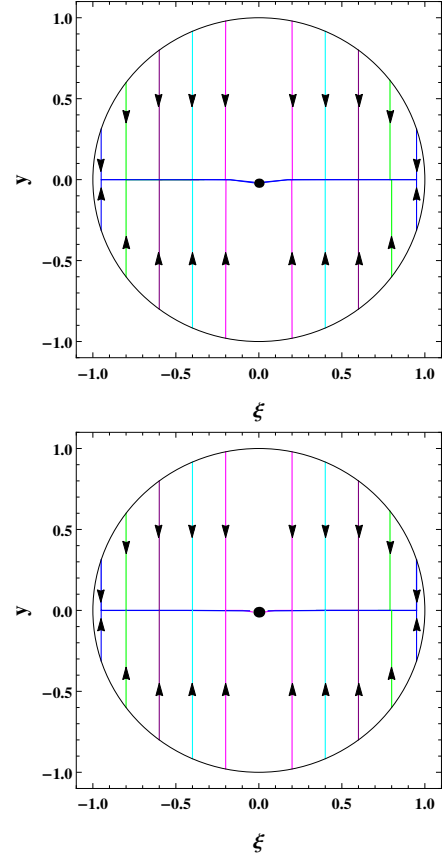


FIG. 12: This figure corresponds to the potential with $n = 2/3$ (Top) and $1/3$ (Bottom). The arrows show the time evolution from boundary to the origin. We use $m = 0.2m_{pl}$.

tor $a(t)$ disappears (see bottom panels of Figs. 1–5). One can get the slow-roll inflation for a long period, and correspondingly a large number of e-folds N_{inf} are obtained, as displayed in bottom panels of Figs. 1–5 and Tables I and II.

Second, we considered NIV at the bounce, in this case also the evolution for KED initial conditions is divided into three regimes, namely bouncing, transition and the slow-roll. The universal feature of expansion factor appears whereas it is lost in case of PED initial conditions. The evolution of $a(t)$, $w(\phi)$ and ϵ_H are shown in Figs. 6–10, and corresponding number of e-folds are presented in Tables III and IV. To be consistent with the current observations at least 60 e-folds are needed during the slow-roll inflation. In case of PIV ($\dot{\phi}_B > 0$), to get at least 60 or more e-folds, we have restricted the range of ϕ_B for $n = 7/4$ and $4/3$ whereas the restriction has disappeared for $n = 1, 2/3$ and $1/3$, see Tables I and II. In contrast, in case of NIV ($\dot{\phi}_B < 0$), all cases of n have restricted range, as shown in Tables III and IV.

We also presented phase space analysis for the inflationary potentials under consideration. As we mentioned, the inflaton field ϕ must be positive in order for the po-

tential to be real. But, it corresponds to only half phase space. Therefore, we used a generic set of dynamical variables to bring out better depiction of underlying dynamics. The phase portraits for the power-law potentials with $n = 7/4, 4/3, 1, 2/3$ and $1/3$ are exhibited in Figs. 11 and 12. Moreover, for the generic initial conditions, the slow-roll inflation is an attractor in the phase space.

Acknowledgements

We would like to thank J.D. Barrow and T. Zhu for valuable discussions and suggestions. A.W. is supported

in part by the National Natural Science Foundation of China (NNSFC) with the Grants Nos. 11375153 and 11675145.

-
- [1] A.H. Guth, Inflationary universe: A possible solution to the horizon and flatness problems, *Phys. Rev.* **D23**, 347 (1981); A.A. Starobinsky, A new type of isotropic cosmological models without singularity, *Phys. Lett.* **B91**, 99 (1980); K. Sato, First-order phase transition of a vacuum and the expansion of the universe, *Mon. Not. R. Astron. Soc.* **195**, 467 (1981).
- [2] P. Collaboration et al., Planck 2015. XX. Constraints on inflation, arXiv:1502.02114 [astro-ph].
- [3] A. Borde and A. Vilenkin, Eternal inflation and the initial singularity, *Phys. Rev. Lett.* **72**, 3305 (1994).
- [4] A. Borde, A. H. Guth, and A. Vilenkin, Inflationary Spacetimes Are Incomplete in Past Directions, *Phys. Rev. Lett.* **90**, 151301 (2003).
- [5] J. Martin, C. Ringeval, and V. Vennin, Encyclopaedia Inflationaris, *Phys. Dark Univ.* **5** (2014) 75 [arXiv:1303.3787].
- [6] J. Martin and R. H. Brandenberger, Trans-Planckian problem of inflationary cosmology, *Phys. Rev.* **D63**, 123501 (2001).
- [7] R. H. Brandenberger and J. Martin, Trans-Planckian issues for inflationary cosmology, *Class. Quantum Grav.* **30**, 113001 (2013).
- [8] Tao Zhu, Anzhong Wang, Gerald Cleaver, Klaus Kirsten, Qin Sheng, Pre-inflationary universe in loop quantum cosmology, *Phys. Rev.* **D 96**, 083520 (2017) [arXiv:1705.07544]; Tao Zhu, Anzhong Wang, Klaus Kirsten, Gerald Cleaver, Qin Sheng, Universal features of quantum bounce in loop quantum cosmology, *Phys. Lett.* **B773** (2017) 196 [arXiv:1607.06329].
- [9] I. Agullo, A. Ashtekar, and W. Nelson, Quantum Gravity Extension of the Inflationary Scenario, *Phys. Rev. Lett.* **109**, 251301 (2012); *Phys. Rev.* **D87**, 043507 (2013).
- [10] I. Agullo, A. Ashtekar, and W. Nelson, The pre-inflationary dynamics of loop quantum cosmology: confronting quantum gravity with observations, *Class. Quantum Grav.* **30**, 085014 (2013).
- [11] I. Agullo and N. A. Morris, Detailed analysis of the predictions of loop quantum cosmology for the primordial power spectra, *Phys. Rev.* **D92**, 124040 (2015).
- [12] A. Ashtekar and P. Singh, Loop quantum cosmology: a status report, *Class. Quantum Grav.* **28**, 213001 (2011).
- [13] A. Ashtekar and A. Barrau, Loop quantum cosmology: from pre-inflationary dynamics to observations, *Class. Quantum Grav.* **32**, 234001 (2015).
- [14] A. Barrau and B. Bolliet, Some conceptual issues in loop quantum cosmology, arXiv:1602.04452.
- [15] J. Yang, Y. Ding, and Y. Ma, Alternative quantization of the Hamiltonian in loop quantum cosmology, *Phys. Lett.* **B682**, 1 (2009).
- [16] A. Ashtekar and D. Sloan, Loop quantum cosmology and slow roll inflation, *Phys. Lett.* **B694**, 108 (2010); Probability of inflation in loop quantum cosmology, *Gen. Relativ. Gravit.* **43**, 3619 (2011).
- [17] P. Singh, K. Vandersloot, and G. V. Vereshchagin, Non-singular bouncing universes in loop quantum cosmology, *Phys. Rev.* **D74**, 043510 (2006); J. Mielczarek, T. Cailleteau, J. Grain, and A. Barrau, Inflation in loop quantum cosmology: Dynamics and spectrum of gravitational waves, *Phys. Rev.* **D81**, 104049 (2010).
- [18] X. Zhang and Y. Ling, Inflationary universe in loop quantum cosmology, *J. Cosmol. Astropart. Phys.* **08**, 012 (2007).
- [19] L. Chen and J.-Y. Zhu, Loop quantum cosmology: the horizon problem and the probability of inflation, *Phys. Rev.* **D92**, 084063 (2015) [arXiv:1510.03135 [gr-qc]].
- [20] B. Bolliet, J. Grain, C. Stahl, L. Linsefors, and A. Barrau, Comparison of primordial tensor power spectra from the deformed algebra and dressed metric approaches in loop quantum cosmology, *Phys. Rev.* **D91**, 084035 (2015).
- [21] S. Schander, A. Barrau, B. Bolliet, L. Linsefors, and J. Grain, Primordial scalar power spectrum from the Euclidean bounce of loop quantum cosmology, *Phys. Rev.* **D93**, 023531 (2016).
- [22] B. Bolliet, A. Barrau, J. Grain, and S. Schander, Observational Exclusion of a Consistent Quantum Cosmology Scenario, *Phys. Rev.* **D93**, 124011 (2016); J. Grain, The perturbed universe in the deformed algebra approach of Loop Quantum Cosmology, *Int. J. Mod. Phys.* **D25**, 1642003 (2016) [arXiv:1606.03271].
- [23] B. Bonga and B. Gupta, Inflation with the Starobinsky potential in Loop Quantum Cosmology, *Gen. Relativ. Gravit.* **48**, 1 (2016); Phenomenological investigation of a quantum gravity extension of inflation with the Starobinsky potential, *Phys. Rev.* **D93**, 063513 (2016).
- [24] J. Mielczarek, Possible observational effects of loop quantum cosmology, *Phys. Rev.* **D81**, 063503 (2010); L. Linsefors, T. Cailleteau, A. Barrau, and J. Grain, Primordial tensor power spectrum in holonomy corrected loop

- quantum cosmology, *Phys. Rev.* **D87**, 107503 (2013); J. Mielczarek, Gravitational waves from the big bounce, *J. Cosmol. Astropart. Phys.* **11**, 011 (2008).
- [25] A. Ashtekar, W. Kaminski, and J. Lewandowski, Quantum field theory on a cosmological, quantum space-time, *Phys. Rev.* **D79** (2009) 064030.
- [26] I. Agullo, A. Ashtekar, and W. Nelson, Quantum Gravity Extension of the Inflationary Scenario, *Phys. Rev. Lett.* **109**, 251301 (2012).
- [27] I. Agullo, A. Ashtekar, and W. Nelson, Extension of the quantum theory of cosmological perturbations to the Planck era, *Phys. Rev.* **D87**, 043507 (2013).
- [28] M. Bojowald, G. M. Hossain, M. Kagan, and S. Shankaranarayanan, Gauge invariant cosmological perturbation equations with corrections from loop quantum gravity, *Phys. Rev.* **D79**, 043505 (2009).
- [29] J. Mielczarek, T. Cailleteau, A. Barrau, and J. Grain, Anomaly-free vector perturbations with holonomy corrections in loop quantum cosmology, *Class. Quant. Grav.* **29**, 085009 (2012) [arXiv:1106.3744].
- [30] T. Cailleteau, J. Mielczarek, A. Barrau, and J. Grain, Anomaly-free scalar perturbations with holonomy corrections in loop quantum cosmology, *Class. Quant. Grav.* **29**, 095010 (2012) [arXiv:1111.3535].
- [31] T. Cailleteau, A. Barrau, J. Grain and F. Vidotto, Consistency of holonomy-corrected scalar, vector and tensor perturbations in Loop Quantum Cosmology, *Phys. Rev.* **D86**, 087301 (2012) [arXiv:1206.6736].
- [32] T. Cailleteau, L. Linsefors, and A. Barrau, Anomaly-free perturbations with inverse-volume and holonomy corrections in loop quantum cosmology, *Class. Quantum Grav.* **31**, 125011 (2014) [arXiv:1307.5238].
- [33] A. Barrau, M. Bojowald, G. Calcagni, J. Grain, and M. Khagan, Anomaly-free cosmological perturbations in effective canonical quantum gravity, *J. Cosmol. Astropart. Phys.* **05** (2015) 051 [arXiv:1404.1018].
- [34] K. Harigaya, M. Ibe, K. Schmitz, and T. T. Yanagida, Chaotic inflation with a fractional power-law potential in strongly coupled gauge theories, *Phys. Lett.* **B720**, 125 (2013); Dynamical fractional chaotic inflation, *Phys. Rev.* **D90**, 123524 (2014).
- [35] J. D. Barrow and A. A. H. Graham, Singular inflation, *Phys. Rev.* **D91**, 083513 (2015); New singularities in unexpected places, *Inter. J. M. Phys.* **D24**, (2015) 1544012.
- [36] E. Silverstein and A. Westphal, Monodromy in the CMB: gravity waves and string inflation, *Phys. Rev.* **D78**, 106003 (2008).
- [37] K. Martineau, A. Barrau and S. Schander, *Phys. Rev.* **D95**, 083507 (2017) [arXiv:1701.02703].
- [38] A. Ashtekar, T. Pawłowski, and P. Singh, *Phys. Rev.* **D74**, 084003 (2006).
- [39] K. A. Meissner, Black hole entropy in loop quantum gravity, *Class. Quantum Grav.* **21**, 5245 (2004).
- [40] M. Domagala, J. Lewandowski, Black hole entropy from quantum geometry, *Class. Quantum Grav.* **21**, 5233 (2004).
- [41] J. Mielczarek, T. Cailleteau, J. Grain, and A. Barrau, Inflation in loop quantum cosmology: Dynamics and spectrum of gravitational waves, *Phys. Rev.* **D81**, 104049 (2010).
- [42] A. A. Starobinsky, A new type of isotropic cosmological models without singularity, *Phys. Lett.* **B91**, 99 (1980).